PHYSICAL REVIEW B **72**, 220507(R) (2005)

Anisotropic temperature-dependent current densities in vicinal $YBa_2Cu_3O_{7-\delta}$

M. Djupmyr,[1] G. Cristiani,[2] H.-U. Habermeier,[2] and J. Albrecht[1,2]
[1]*Max-Planck-Institut für Metallforschung, Heisenbergstrasse 3, D-70569 Stuttgart, Germany*
[2]*Max-Planck-Institut für Festkörperforschung, Heisenbergstrasse 1, D-70569 Stuttgart, Germany*
(Received 29 September 2005; published 20 December 2005)

Thin epitaxial films of $YBa_2Cu_3O_{7-\delta}$ grown on vicinal cut substrates exhibit a substantial anisotropy of the critical current density j_c in the film plane. By means of a quantitative magneto-optical analysis it is possible to investigate the current densities along different directions independently from each other. We performed a detailed analysis of the temperature dependence of the critical currents in the range $T=5-90$ K and found a completely different behavior of $j_c(T)$ along different directions. Describing the data by a step-wise power-law ansatz allows us to distinguish between different current limiting mechanisms.

DOI: 10.1103/PhysRevB.72.220507 PACS number(s): 74.25.Qt, 74.25.Sv, 74.72.Bk, 74.78.Bz

Many possible applications for high-temperature superconductors, such as current carrying tapes, electronic filters, or magnetic field sensors are going to be realized using thin epitaxial films.[1–4] Especially for the transport of electric currents it is desirable to create materials with high critical current densities. Thin epitaxial films of $YBa_2Cu_3O_{7-\delta}$ (YBCO) can exhibit current densities of up to 8×10^{11} A/m^2 at low temperatures due to defect structures that allow effective flux line pinning.[5,6] It could be shown that the critical current densities in epitaxial YBCO films are also related to the properties of the coalescence region of the growth islands.[7] An elegant method to distinguish between different mechanisms limiting the current transport is given by the detailed analysis of the temperature dependence of the critical current density.[7–11] Owing to the fact that the quality of the boundaries between growth islands plays a decisive role for current transport, at least at low temperatures,[7] it is interesting to study YBCO films on vicinal cut substrates. The steps of the vicinal cut substrate restrain the island growth and instead a self-organizing step-flow growth occurs.[12] This makes it possible to produce films with few grain boundaries in the direction of the steps, though instead an array of antiphase boundaries are formed along the step edges. Due to the antiphase boundaries the magnetic flux penetration is anisotropic and the critical current along the steps is higher than across the steps.[13,14] Measurements of the current component flowing along the steps can give information about a system without growth-induced grain boundaries.

Thin films of optimally doped YBCO grown on vicinal cut $SrTiO_3$ (106) substrates were studied. The miscut of the substrate towards the (100) direction was $\theta=9.46°$. This angle produces steps with a width $w=a_{STO}/\tan\theta=11$ nm which is a multiple of $a_{STO}=3.905$ Å, the lattice constant of $SrTiO_3$. This results in very straight steps with heights of one unit cell.[13,15] 5×5 mm^2 YBCO films are grown onto these substrates using pulsed laser deposition with nominal thicknesses of 150 nm. The steps in the substrate lead to a step flow growth of YBCO ending up in a very homogeneous film, containing no islands along the steps.[12] In-between the steps there is a stacking mismatch of the YBCO lattice producing nearly parallel antiphase boundaries (APB) that are elongated along the steps and are parallel to the c axis. This has been shown using scanning tunneling microscopy and transmission electron microscopy on samples grown in the same setup and thus showing similar properties as the film used here.[13,15] It has also been seen that the twinning is partially suppressed so that about 70% of the YBCO has the *b* axis oriented along the steps.[16] Because of the defect free growth, the APB's are expected to dominate as pinning sites.[17]

The penetration of magnetic flux into these films is investigated using the magneto-optical Faraday effect. This allows the direct imaging of the magnetic flux density distribution.[18] A ferrimagnetic lutetium-doped iron garnet film is used as a field sensing layer.[19] That, together with a polarization light microscope combined with a charge-coupled device camera, gives a spatial resolution of up to 1 μm and a magnetic resolution of better than 1 mT. From the so produced gray-scale images of the magnetic flux distribution, the critical current density can be calculated using an inversion scheme of the Biot Savart law. In the film we assume a two-dimensional current density distribution, which makes the inversion unambiguous.[20] There is an in-plane component of the external magnetic field caused by the supercurrents. This has to be omitted wherefore an iteration method developed by Laviano *et al.*,[21] has been used. The resulting current density distributions have a spatial resolution of about 5 μm.

In our experiment, the film was cooled down to $T\approx5$ K in an external field of $\mu_0H\approx250$ mT. Then, the field was removed to put the sample into the remanent state. The images of the flux distribution were then taken at increasing temperatures, from 6.5 K to above $T_c=91$ K. To take care of the relaxation processes of the vortices,[22] a constant delay time of 10 s was used before acquiring each image.

Figure 1(a) schematically shows the directions of the currents in the film, given as longitudinal (L) along and transversal (T) across the APBs, or the steps of the substrate, indicated by the vertical solid lines in the figure.

The quantitative flux distribution at 20 K is shown in Fig. 1(b) as a gray-scale image together with the numerically calculated current streamlines showing the current path in the sample. The gray-scale image represents B_z, the flux density component perpendicular to the surface of the film, with bright parts referring to a high local flux density of about 20 mT. The current is flowing in nicely shaped rectangular loops parallel to the film edges. Figure 1(c) shows the corresponding modulus of the critical current distribution for the film, calculated as described above. The current density profile

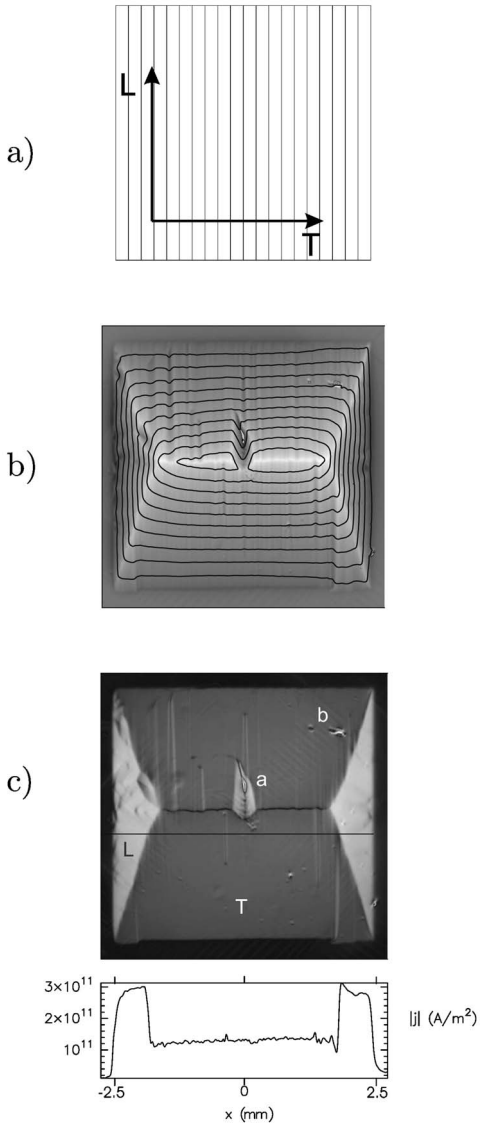

FIG. 1. Square shaped YBCO film grown on vicinal cut $SrTiO_3$. The images were taken at 20 K. (a) Sketch of the L and T directions of the currents in relation to the steps of the substrate. (b) Magneto-optical image of the magnetic flux distribution and the calculated current stream lines. (c) The critical current distribution as calculated from 1(b) and a current density profile taken along the black line.

below the image is taken at the solid black line. The strong anisotropy of j_c due to the steps is clearly seen as different current densities in the regions with different current directions, higher in the L direction (light gray), lower in the T direction (dark gray). At a temperature of $T=20$ K the different directions show critical current densities of $j_{c,L}=2.8\times10^{11}$ A/m^2 and $j_{c,T}=1.2\times10^{11}$ A/m^2, respectively. These are typical values for high quality 150 nm thick YBCO films grown on vicinal $SrTiO_3$.[6,23] Two macroscopic irregularities in the film are marked out in the picture. At (a), there is a scratch in the film resulting in an area which cannot be crossed by the supercurrents. The currents are forced to flow around the scratch resulting in components along the APB's

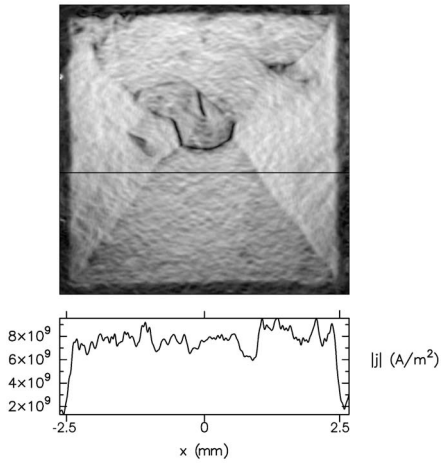

FIG. 2. The critical current density distribution at 89 K and a current density profile taken along the black line.

and, thus, in an enhanced current density in that area. The white spot marked with (b) refers to a defect in the detector layer and is not related to superconducting properties. Apart from these the film is nearly defect free and of a high quality supported by the high values for the critical current densities especially in the L direction.

As a comparison, the critical current distribution in the same film at $T=89$ K is shown in Fig. 2. At this temperature the critical current is reduced to about $j_c=8\times10^9$ A/m^2 and the difference between the two directions is very small. Also the angle between the discontinuity lines and the film edge has increased and almost a cross is formed, like in films on flat substrates.[24] This means, that the anisotropy of the film has almost disappeared at this temperature close to T_c.

To investigate the temperature-dependent properties of the film in more detail, the critical current densities are determined for temperatures from $T=6.5$ K to $T=90$ K. The critical currents are averaged over an area with side lengths of several 100 μm for each current direction. To take care of a possible field dependence of the critical current due to flux-line flux-line interactions, these areas were chosen to be around the $B=0$ line, that necessarily appears in the remanent state.[25] These carefully obtained temperature dependences of the critical currents are depicted in Fig. 3, showing very different behavior for the two directions. The current in the L direction, squares, shows a similar behavior as those previously found in epitaxial films and films with improved microstructure[7] as well as for low-angle grain boundaries.[10] The T direction, circles, on the other hand, shows a completely different behavior.

In a first analysis we have a look at the temperature where j_c is vanishing. This temperature for both directions can be estimated by a linear fit to the values at higher temperatures, seen in the inset of Fig. 3. For both directions we find values close to $T\approx91$ K which means that there is no substantial suppression of T_c due to the antiphase boundaries. The anisotropy ratio A_j of the critical current density for low temperatures is $A_j=j_{c,L}/j_{c,T}=2.5$. With increasing temperature the anisotropy decreases to disappear completely at T_c.

The Ginzburg-Landau theory suggests an ansatz for describing the temperature dependence of the critical current

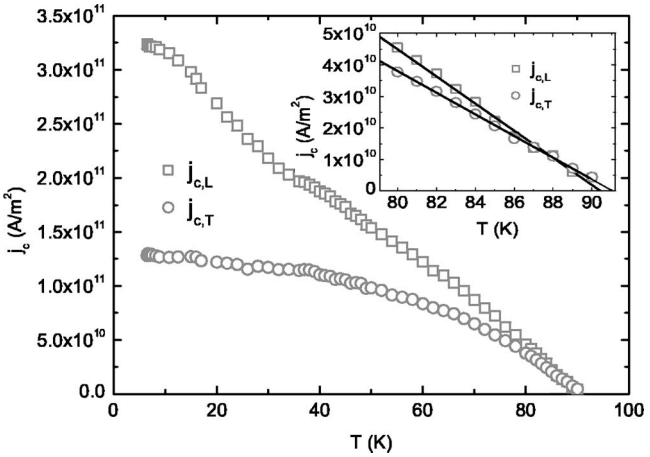

FIG. 3. Temperature dependence of the critical currents in YBCO grown on a vicinal cut $SrTiO_3$ substrate. $j_{c,L}$ (□) is the longitudinal current density along and $j_{c,T}$ (○) the transversal across the APB's. The inset shows linear fits to the data close to T_c.

density for different systems. The two characteristic lengths of a superconductor, the coherence length ξ and the London penetration depth λ show temperature dependences of λ, $\xi \propto (1-T/T_c)^{-1/2}$ for T close to T_c. This motivates an ansatz for the critical current density

$$j_c \propto j_0(1 - T/T_c)^s. \quad (1)$$

If this power law can describe the data reasonably is checked by plotting the data as j_c over $1-T/T_c$ using double logarithmic scaling. In Fig. 4 the data for the L direction is shown. The errors are estimated not to be greater than 3×10^9 A/m^2 and are shown in the diagram. The data can be fitted to Eq. (1) using j_0 and s as free parameters. For temperatures above $T \approx 40$ K as can be seen in Fig. 4 the fit gives $s=0.9$. At the temperature $T=40$ K the slope changes and one finds $s=1.4$ for lower temperatures, see Fig. 5. For

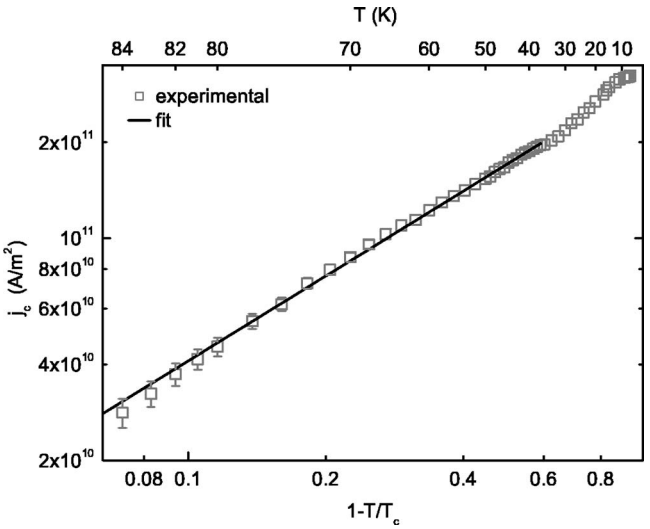

FIG. 4. Temperature dependence of the longitudinal critical current density $j_{c,L}$. The line represents a fit to the power law $j_c \propto (1-T/T_c)^s$ with $s=0.9$.

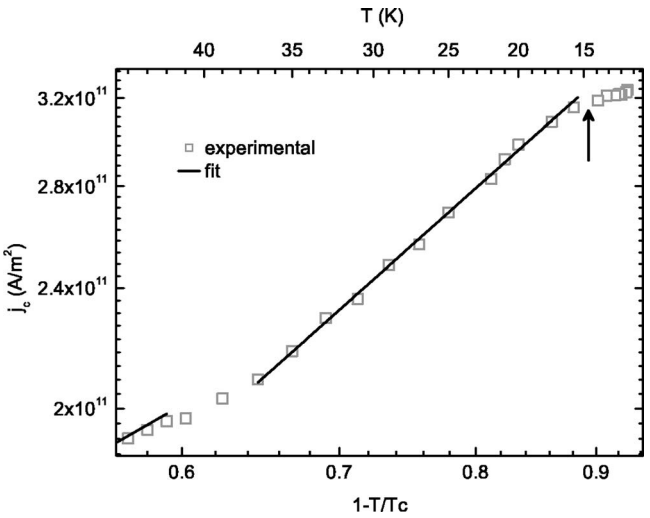

FIG. 5. Temperature dependence of the longitudinal critical current density $j_{c,L}$ for temperatures up to 50 K. The line represents a fit to the power law $j_c \propto (1-T/T_c)^s$ with $s=1.4$. The arrow indicates the temperature below which a deviation from the powerlaw occurs.

both temperature regimes the fit is able to describe the experimental data well and a two-step power-law behavior is found. The power-law ansatz works properly down to temperatures of $T=15$ K. Here a significant deviation occurs, indicated by the arrow in Fig. 5. This finding can possibly be explained by the onset of quantum creep of vortices at low temperatures.[26] The temperature dependence in the T direction, Fig. 6 looks very different, though also here the value $s=0.9$ is found at higher temperatures. Below $T=70$ K the slope of the curve becomes continuously smaller and nearly runs into a saturation value of $j_c \approx 1.3 \times 10^{11}$ A/m^2 at low temperatures. This behavior is unusual for epitaxially grown YBCO films without weak links, that can be ruled out due to the high critical currents. A qualitatively similar behavior is found for tunneling currents across SIS contacts in classical superconductors, described by Ambegaokar and Baratoff.[27]

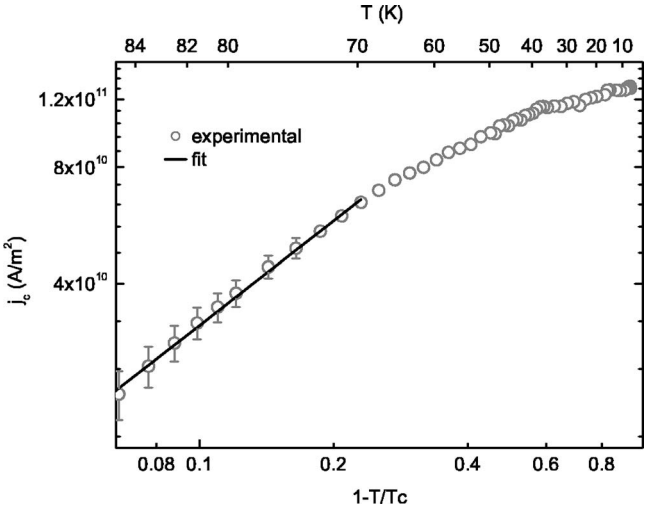

FIG. 6. Temperature dependence of the transversal critical current density $j_{c,T}$. The line represents a fit to the power law $j_c \propto (1-T/T_c)^s$ with $s=0.9$.

The experimental data have been obtained at low flux densities making it possible to discuss the results within the frame of individual flux line pinning. Considering flux-line core pinning, the condensation energy per unit length of the flux line is given by $\epsilon(T)=\Phi_0^2/[8\pi\mu_0\lambda^2(T)]$ where the temperature dependence only comes in through λ. The coherence length ξ describing the length over which this energy can vary is connected to $\lambda(T)=\kappa\xi(T)$, where κ is the Ginzburg-Landau parameter. The temperature dependence of the coherence length $\xi\propto(1-T/T_c)^{-1/2}$ thus leads to $\epsilon(T)=\epsilon_0(1-T/T_c)$. In case of thermal depinning, the flux line has to overcome an activation energy that is proportional to ϵ. Thus the expected temperature dependence for the critical current density is $j_c(T)=j_0(1-T/T_c)$, the exponent being $s=1$. For the measured films on vicinal cut substrates, at temperatures above $T=40$ K (L direction) and $T=70$ K (T direction), both current directions show the same exponent $s=0.9$, which is close to $s=1$. Also, the values found in films with different microstructure[7] and for single grain boundaries[10] were close, $s=1.1$ and $s=1.2$, respectively. This suggests that for higher temperatures thermally activated depinning of the flux lines acts as a limiting factor for the critical current density.

At $T\approx 40$ K the power law describing $j_{c,L}(T)$ changes and the exponent is found to be $s=1.4$ indicating a change of the flux pinning properties. At lower temperatures, thermally activated depinning plays a minor role and the flux pinning is instead governed by the maximum pinning force. This force is given by the gradient of the pinning potential, which means the shape of the potential at the pinning sites is more important than the depth. Different values of the exponent s have been found for films with different grain-boundary structures. An exponent of $s=3.0$ is found for a film containing a single, well-defined grain boundary with 3° misorientation. For a standard epitaxial film $s=2$ is found and for films with improved grain boundaries, $s=1.7$. Following this, for a film grown on a vicinal cut substrate, the even lower value of $s=1.4$ found for the L direction can be explained by the reduced density of grain boundaries. This due to the step-flow growth of the film resulting in absence of island formation. The found exponent $s=1.4$ is close to $s=\frac{3}{2}$, a temperature dependence that is also found for the depairing current density $j_0=c\Phi_0/12\sqrt{3}\pi^2\lambda^2\xi\propto(1-T/T_c)^{3/2}$ in Ginzburg-Landau theory.

Summarizing, using the quantitative magneto-optical Faraday effect it was possible to study the temperature dependence of the critical current densities independently for both occurring current directions. The measurements could be performed with high accuracy up to $T=90$ K. The current flowing parallel to the steps, $j_{c,L}(T)$ shows a behavior which can be described by a two-step power-law ansatz. For $T>40$ K, $s=0.9$ is found, suggesting thermal depinning to be the current limiting mechanism while for $T<40$ K with $s=1.4$, the behavior follows that of the depairing current. The current direction $j_{c,T}(T)$ shows a behavior characteristic for SIS tunneling, although near T_c also here a nearly linear behavior is found.

[1] D. Larbalestier, A. Gurevich, D. Feldmann, and A. Polyanskii, Nature (London) **414**, 368 (2001).
[2] N. Klein, Rep. Prog. Phys. **65**, 1387 (2002).
[3] D. Koelle, R. Kleiner, F. Ludwig, E. Dantsker, and J. Clarke, Rev. Mod. Phys. **71**, 631 (1999).
[4] A. Malozemoff, J. Mannhart, and D. Scalapino, Phys. Today **58** (4), 41 (2005).
[5] B. Dam, J. Huijbregtse, F. Klaassen, R. van der Geest, G. Doornbos, J. Rector, A. Testa, S. Freisem, J. Martinez, B. Stäuble-Pümpin, and R. Griessen, Nature (London) **399**, 439 (1999).
[6] C. Jooss, R. Warthmann, and H. Kronmüller, Phys. Rev. B **61**, 12433 (2000).
[7] S. Brück and J. Albrecht, Phys. Rev. B **71**, 174508 (2005).
[8] J. Mannhart, P. Chaudhari, D. Dimos, C. C. Tsuei, and T. R. McGuire, Phys. Rev. Lett. **61**, 2476 (1988).
[9] H. Darhmaoui and J. Jung, Phys. Rev. B **53**, 14621 (1996).
[10] J. Albrecht, Phys. Rev. B **68**, 054508 (2003).
[11] H. Yan, M. M. Abdelhadi, J. A. Jung, B. A. Willemsen, and K. E. Kihlstrom, Phys. Rev. B **72**, 064522 (2005).
[12] F. Wellhöfer, P. Woodall, D. Norris, S. Johnson, D. Vassiloyannis, M. Aindow, M. Slaski, and C. Muirhead, Appl. Surf. Sci. **127–129**, 525 (1998).
[13] T. Haage, J. Zegenhagen, J. Q. Li, H.-U. Habermeier, M. Cardona, C. Jooss, R. Warthmann, A. Forkl, and H. Kronmüller, Phys. Rev. B **56**, 8404 (1997).
[14] J. H. Durrell, G. Burnell, V. N. Tsaneva, Z. H. Barber, M. G. Blamire, and J. E. Evetts, Phys. Rev. B **70**, 214508 (2004).
[15] T. Haage, J. Li, B. Leibold, M. Cardona, J. Zegenhagen, H.-U. Habermeier, A. Forkl, C. Jooss, R. Warthmann, and H. Kronmüller, Solid State Commun. **99**, 553 (1996).
[16] J. Brötz, H. Fuess, T. Haage, and J. Zegenhagen, Phys. Rev. B **57**, 3679 (1998).
[17] C. Jooss, R. Warthmann, H. Kronmüller, T. Haage, H.-U. Habermeier, and J. Zegenhagen, Phys. Rev. Lett. **82**, 632 (1999).
[18] C. Jooss, J. Albrecht, H. Kuhn, S. Leonhardt, and H. Kronmüller, Rep. Prog. Phys. **65**, 651 (2002).
[19] L. Dorosinskii, M. Indenbom, V. Nikitenko, Y. Ossip'yan, A. Polyanskii, and V. Vlasko-Vlasov, Physica C **203**, 149 (1992).
[20] C. Jooss, R. Warthmann, A. Forkl, and H. Kronmüller, Physica C **299**, 215 (1998).
[21] F. Laviano, D. Botta, A. Chiodoni, R. Gerbaldo, G. Ghigo, L. Gozzelino, S. Zannella, and E. Mezzetti, Supercond. Sci. Technol. **16**, 71 (2003).
[22] R. Warthmann, J. Albrecht, H. Kronmüller, and C. Jooss, Phys. Rev. B **62**, 15226 (2000).
[23] C. Jooss and J. Albrecht, Z. Metallkd. **93**, 1065 (2002).
[24] T. Schuster, M. V. Indenbom, M. R. Koblischka, H. Kuhn, and H. Kronmüller, Phys. Rev. B **49**, 3443 (1994).
[25] T. Schuster, M. Koblischka, H. Kuhn, B. Ludescher, M. Leghissa, M. Lippert, and H. Kronmüller, Physica C **196**, 373 (1992).
[26] H. Wen, H. Schnack, R. Griessen, B. Dam, and J. Rector, Physica C **241**, 353 (1995).
[27] V. Ambegaokar and A. Baratoff, Phys. Rev. Lett. **10**, 486 (1963).